Journal of Electroanalytical Chemistry 780 (2016) 271–275

Contents lists available at ScienceDirect

Journal of Electroanalytical Chemistry

journal homepage: www.elsevier.com/locate/jelechem

# Effect of ZnS interfacial passivation layer to CdS quantum dot-sensitized ZnO nanorods

Chunyan Zhou, Qian Chen, Guofang Wang, Anxiang Guan, Liya Zhou *, Ni Huang, Jiehua Xu

*School of Chemistry and Chemical Engineering, Guangxi University, Nanning 530004, China*

ARTICLE INFO

*Article history:*
Received 2 May 2016
Received in revised form 23 September 2016
Accepted 24 September 2016
Available online 26 September 2016

*Keywords:*
ZnS interfacial passivation
CdS quantum dots
ZnO nanorods

ABSTRACT

ZnS interfacial passivation layer was coated on ZnO nanorods (NRs) fabricated by one-step hydrothermal technique via successive ionic layer adsorption and reaction (SILAR). The ZnO NRs were further sensitized by CdS quantum dots (QDs) as a photoanode of QD-sensitized solar cells (QDSSCs). The effect of the ZnS interfacial passivation layer on the performance of the QDSSCs was systematically investigated by varying the SILAR cycle number. The ZnS layer with an appreciated thickness not only suppressed the recombination of injected electrons with holes on the CdS QDs but also effectively passivated the surface trap states of ZnO NRs and increased the deposition of CdS QDs. These characteristics improved the light-harvesting efficiency of the photoelectrode. The conversion efficiency of the CdS QD-sensitized ZnO NRs with ZnS interfacial passivation layer could reach a maximum of 1.53%, which was enhanced by 300% compared with that of the cell based on CdS QD-sensitized ZnO NRs (0.51%).



## 1. Introduction

Zinc oxide (ZnO) is a wide-band gap (3.37 eV) metal oxide with high exciton binding energy and has better electron mobility (115–155 $cm^2 V^{-1} S^{-1}$) than $TiO_2$ ($10^{-5}$ $cm^2 V^{-1} S^{-1}$) [1,2]. This compound has been investigated extensively because of its important application in various fields as a solar cell [3–5], photocatalyst [6], and optical device [7]. However, the intrinsic band gap of ZnO and high recombination rate of electron–hole pairs limit the further improvement of its photoelectrochemical properties. Various promising semiconductor quantum dots (QDs), such as CdS [8,9], CdSe [10], CdTe [11], and PbS [12,13], have been deposited on ZnO to overcome these drawbacks. The QDs are beneficial because of their high stability, multiple exciton generation, large intrinsic dipole moments [14–16], etc. Compared with other materials, CdS is an important direct-band semiconductor with a bandgap of 2.42 eV toward ZnO NRs (NRs); CdS is also reported to be stable with high compatibility and electron transfer rate [17]. Thus, CdS has been considered for potential application in photovoltaic and photosensitive devices.

Numerous methods for CdS QD deposition on ZnO surface have been reported. These methods include hydrothermal method, successive ionic layer adsorption and reaction (SILAR), chemical bath deposition, sol-gel, and microwave-assisted method [18–20]. CdS-modified ZnO is often used as photoanode material for solar cells. The semiconductor layer with highly negative conducting band (CB) and high conduction band edge is usually coated on the surface of QD-sensitized semiconductor to suppress the recombination of charge carriers from the sensitizer and ZnO to the electrolyte solution [21,22]. For example, the CB for three materials with ZnS layer on CdS QD-sensitized ZnO NRs increases in the following order to form a stepwise structure of the band edge: ZnO < CdS < ZnS. Consequently, the ZnS interfacial passivation layer on the ZnO NRs blocks the injected electrons on ZnO NRs to recombine with hole on CdS QDs, increasing the photovoltaic performance of QD-sensitized solar cells (QDSSCs).

A barrier layer of ZnS deposited onto the CdS surface has been reported to enhance the stability of QDSSC and inhibit the corrosion of CdS QDs [22,23]. However, few studies have reported the effect of ZnS interfacial passivation layer on cell performance. Hsu et al. [24] studied ZnS passivation layer to CdS-sensitized vertically aligned single-crystal $TiO_2$ NRs on transparent conducting glass with improved solar cell efficiency and stability. Jiang et al. [25] developed uniform ZnO/ZnS/CdS NR films with ion-exchange approach.

This study was performed to investigate the effect of ZnS interfacial passivation layer on the photovoltaic performance of the QDSSCs by varying the amount of ZnS (SILAR cycle number). ZnO NRs were fabricated by one-step hydrothermal technique and passivated with ZnS interfacial layer via SILAR. Then, the NRs were further sensitized by CdS QDs by direct adsorption (DA) method as a photoanode of QDSSCs. The energy band diagram of photoanode in this structure is illustrated in Fig. 1.

## 2. Experimental

### 2.1. Hydrothermal synthesis of ZnO NRs

Fluorine-doped tin oxide (FTO, 10 $\Omega/cm^2$) sheet glass was used as the substrate. Ethyl alcohol with 0.05 M $Zn(Ac)_2 \cdot 2H_2O$ and 0.05 M diethanol amine was prepared as the seed solution. The substrates

* Corresponding author.
*E-mail address:* zhouliyatf@163.com (L. Zhou).

http://dx.doi.org/10.1016/j.jelechem.2016.09.039
1572-6657/

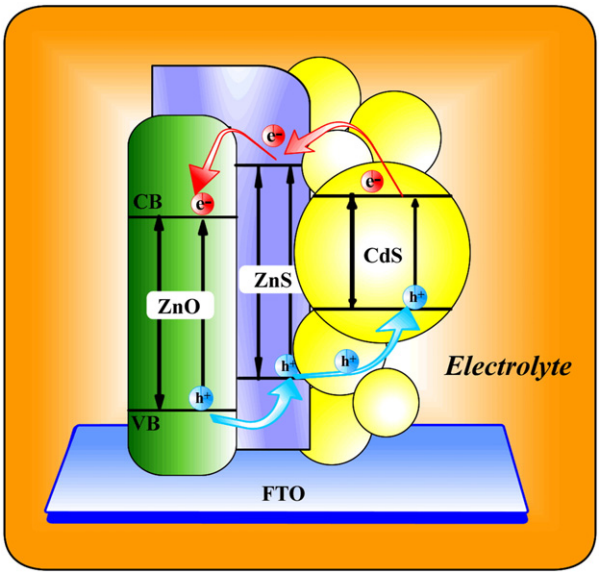


**Fig. 1.** Energy band diagram of CdS/ZnS/ZnO photoanode.

were immersed into the seed solution for 10 s and then annealed at 400 °C for 2 min to form ZnO nanoparticles as the seed layer. ZnO NRs were prepared on the FTO substrates by one-step hydrothermal method. Ammonia (25%, 12 mL) and 240 mL of 0.1 M zinc acetate solution were evenly mixed as a reaction solution and then poured into teflon bottles with autoclavable screw caps. The FTO substrates were then dipped into the solution with the conductive side facing up, and the closed bottles were heated at 90 °C for 180 min. The samples were taken out, rinsed with deionized water, and dried in air at room temperature.

### 2.2. Preparation of CdS QDs

Mercaptopropanoic acid (MPA)-capped CdS QDs were prepared using one-pot aqueous method. MPA (0.3 mL) was added to 100 mL of 0.02 mol/L $CdCl_2 \cdot 2.5H_2O$ solution while stirring. $Na_2S \cdot 9H_2O$ was injected into the solution after the pH of the solution was adjusted to 10.54. The typical molar ratio of $Cd^{2+}/S^{2-}$/MPA was 1:0.2:2.14. The resulting mixture solution was heated to 100 °C for 3 h.

### 2.3. Interfacial treatment and surface sensitization of ZnO NRs

The ZnS layer was modified on the surface of the as-prepared ZnO NRs using SILAR. The ZnO thin film electrode was dipped in 0.1 M $Zn(Ac)_2$ solution for 3 min, washed with water thoroughly, followed by dipping in 0.1 M $Na_2S$ solution for 5 min and washing with water. This procedure was deemed as 1 cycle, which was repeated 3, 6, 9, 12 and 15 times, and the corresponding products were denoted as ZnS(3)/ZnO, ZnS(6)/ZnO, ZnS(9)/ZnO, ZnS(12)/ZnO, and ZnS(15)/ZnO. Then, CdS/ZnS/ZnO samples were prepared by DA for use as photoanode, and deposition was performed at 60 °C for 6 h.

### 2.4. Characterization of QD-sensitized ZnO NRs

The structures were measured by a Bruker/D8 Advance X-ray diffractometer (XRD). High-resolution transmission electron microscope (HRTEM) images, morphologies and elemental compositions of the sample were determined using a scanning electron microscope (JEOL-2100F) with an energy-dispersive spectrometer (HitachiS-3400N). The UV–visible absorption and photoluminescence (PL) spectra of the samples were recorded using UV-2501PC and RF-5301 fluorescence spectrometers, respectively. Brunauer–Emmett–Teller method (BET) specific surface area was measured by nitrogen adsorption at 77 K on a Micromeritics NOVA 3000 adsorption apparatus. The photocurrent–voltage ($J$–$V$) and photocurrent–time ($J$–$t$) curves were measured under illumination by a solar simulator at 1 sun (AM 1.5, 100 mW/cm$^2$) with a saturated Ag/AgCl reference electrode, Pt counter electrode, and polysulfide electrolyte composed of 0.5 M $Na_2S$ and 0.7 M $Na_2SO_3$. Incident photon-to-current conversion efficiency (IPCE) was measured by a Zolix electrochemical station using a Zolix LSH-X150 150-W Xe lamp combined with a monochromator.

## 3. Results and discussion

The energy band diagram of CdS/ZnS/ZnO NRs photoanodes is shown in Fig. 1. The band alignment facilitated the transportation of both electrons and holes in this structure. The elevation of the CB of ZnS was higher than that of ZnO. Thus, the electrons created in ZnS could be transferred to ZnO. In addition, the presence of this ZnS intermediate layer efficiently inhibited the transportation of electrons in the opposite direction and the probability of electron–hole recombination. Thus, the dark current density was reduced, and the photocurrent conversion efficiency (PCE) increased.

Fig. 2 shows the XRD patterns of the phase structures of the ZnO NRs with modified and unmodified QDs. Five main diffraction peaks of the pure ZnO NRs could be indexed to the (100), (002), (101), (110), and (103) planes of the hexagonal-phase (wurtzite structure) ZnO (JCPDS Card No. 36-1451). The inset in Fig. 2 indicates the CdS/ZnS/ZnO NRs marked by a circle, which clearly demonstrates that QDs were successfully formed along with the ZnO NRs.

Fig. 3(a–c) shows the scanning electron micrographs of ZnO NRs, ZnS(9)/ZnO NRs, and CdS/ZnS(9)/ZnO NRs. Fig. 3(a) shows the image of bare ZnO NRs with tip diameters of approximately 300 nm, lengths of approximately 3–5 μm, and smooth surfaces. Then, the deposition of ZnS and CdS via SILAR and DA resulted in the rough surface of ZnO NRs compared with bare ZnO NRs (Fig. 3b and c). This result indicates that the CdS and ZnS QDs were well coated onto ZnO NRs. The energy-dispersive spectrum of the CdS/ZnS(9)/ZnO NRs is presented in Fig. 3(d), demonstrating the presence of Zn, O, Cd, and S. The structures of the as-prepared samples are further demonstrated by their TEM and HRTEM images in Fig. 3(e) and (f). Fig. 3(e) shows the typical TEM image of ZnS(9)/ZnO NR, the core-shell structure can be seen clearly with the thickness of shell layer of 21–25 nm. The crystalline structure of CdS/ZnS(9)/ZnO NR is shown by a HRTEM image in Fig. 4(f). The fringe spacing of 0.26 nm in the single-crystalline core matches well the interplanar spacing of the (002) plane of hexagonal ZnO, while fringe spacing of 0.31 nm and 0.33 nm in the polycrystalline shell matches well to interplanar spacing of the (111) plane of cubic ZnS

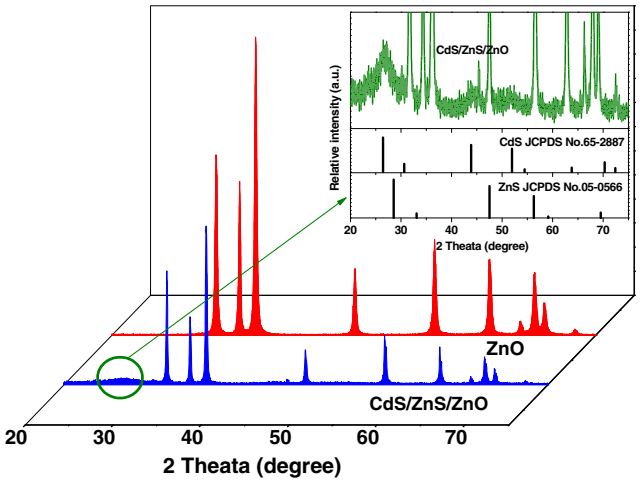


**Fig. 2.** XRD of ZnS layer to CdS QD-sensitized ZnO NRs.